

SLS-TME-TA-2002-0206
9th August 2002

First Operation of the Swiss Light Source

M. Böge

Paul Scherrer Institut, CH-5232 Villigen PSI, Switzerland

Abstract

The Swiss Light Source (SLS) at the Paul Scherrer Institute (PSI) is the most recent 3rd generation light source to be commissioned. It consists of a 100 MeV linac, a novel type of full energy booster synchrotron and a 12-TBA storage ring of 288 m circumference providing 5 nm rad natural emittance at 2.4 GeV. The SLS project was approved by the Swiss Government in September 1997. Commissioning of the SLS began in January 2000 and was successfully completed to within design specifications in August 2001. 70 % of beam time has since been dedicated to the operation of the first four beamlines. Key design features are reviewed and the main commissioning results presented, including that of innovative subsystems such as the digital BPM system, the digital power supplies, the high stability injection system and the first insertion devices. A report on the initial operation experience is also given.

*Presented at the 8th European Particle Accelerator Conference (EPAC'02)
3-7 June 2002, La Villette-Paris, France*

FIRST OPERATION OF THE SWISS LIGHT SOURCE

M. Böge, PSI, Villigen, Switzerland

Abstract

The Swiss Light Source (SLS) at the Paul Scherrer Institute (PSI) is the most recent 3rd generation light source to be commissioned. It consists of a 100 MeV linac, a novel type of full energy booster synchrotron and a 12-TBA storage ring of 288 m circumference providing 5 nm rad natural emittance at 2.4 GeV. The SLS project was approved by the Swiss Government in September 1997. Commissioning of the SLS began in January 2000 and was successfully completed to within design specifications in August 2001. 70 % of beam time has since been dedicated to the operation of the first four beamlines. Key design features are reviewed and the main commissioning results presented, including that of innovative subsystems such as the digital BPM system, the digital power supplies, the high stability injection system and the first insertion devices. A report on the initial operation experience is also given.

1 TIME SCHEDULE

The SLS project was approved by the Swiss Government in September 1997. By June 1999 the building was erected. Commissioning of the SLS 100 MeV linac [1] and the 2.7 GeV booster synchrotron [2] was successfully completed to within design specifications during the period of January-April and July-September 2000. First stored beam in the storage ring [3] was obtained by December 15 2000. By June 2001 storage ring commissioning had entered its final phase by reaching the design current of 400 mA. Excellent agreement of lattice functions with design calculations could be achieved and first undulator spectra were measured [4, 5]. As scheduled, from August 2001 the SLS could dedicate 70 % of the operation time to users, serving four beamlines by the end of 2001. From January-April 2002, 1300 operating hours had been provided to users, with an average availability of 90 % accumulating an integrated beam current of ≈ 250 Ah.

2 THE INJECTORS

2.1 Booster Synchrotron

The main injector is a novel type of full energy booster synchrotron operating up to a maximum energy of 2.7 GeV. Instead of building a booster with a compact lattice the SLS booster is mounted to the inner wall of the storage ring tunnel (see Fig. 1). This allows to distribute the total bending field over a large number of small magnets. The chosen design features a number of advantages:

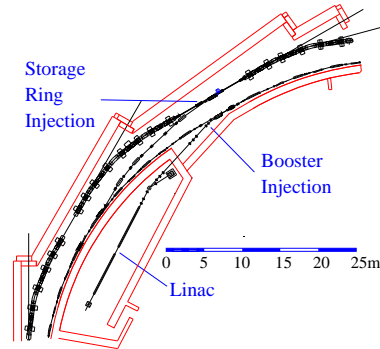


Figure 1: Layout of the tunnel, showing the linac, booster, storage ring and corresponding transfer lines

- substantial saving on building space and shielding
- low field magnets with small apertures
- simple stainless steel vacuum chamber
- low power consumption (< 200 kW at 3 Hz and < 30 kW for continuous top-up injection)
- flexible repetition rates and field ramping modes including the operation as a storage ring < 1.7 GeV
- low emittance beam (9 nm rad at extraction energy of 2.4 GeV), clean injection into the storage ring
- simple booster-ring transfer line

Maximum Energy	GeV	2.7
Circumference	m	270
Lattice		FODO with 3 straights of 8.68 m
Harmonic number		(15x30)=450
RF frequency	MHz	500
Peak R F voltage	MV	0.5
Maximum current	mA	12
Maximum rep. Rate	Hz	3
Tunes		12.39 / 8.35
Chromaticities		-1 / -1
Momentum compaction		0.005
Equilibrium values at 2.4 GeV		
Emittance	nm rad	9
Radiation loss	keV/turn	233
Energy spread, rms		0.075 %
Partition numbers (x,y, ϵ)		(1.7, 1, 1.3)
Damping times (x,y, ϵ)	ms	(11, 19, 14)

Table 1: Booster synchrotron parameters

Limiting the maximum repetition rate to 3 Hz leads to low eddy currents induced in the vacuum chamber and thus allows to have a simple chamber design where a round stainless steel tube of 0.7 mm thickness deforms into an elliptical cross-section of 30-20 mm² requiring no reinforcement. Nevertheless the rate is sufficient to fill the storage ring within 2-3 min. The relevant parameters of the booster are summarized in Table 1. The only “drawback” of the booster concept is a relatively large number of components.

The SLS booster consists of 93 combined function magnets, 18 quadrupoles, 18 sextupoles, 108 corrector magnets and 97 pumping stations. The basic structure of the lattice is defined by three arcs each followed by a 8.68 m long dispersion free straight section. One arc consists of two matching plus 13 FODO cells with $\approx 90^\circ/60^\circ$ phase advance, which contain two focussing/defocussing combined function magnets separated by 1.44 m drifts. These magnets are connected through a single power supply circuit. Residual field differences are compensated by means of a trim coil. Although a basic chromaticity correction is already provided by the profile of the booster dipole, two sextupoles families with three pairs/arc add flexibility to the chromaticity correction. The FODO-lattice has surprisingly relaxed tolerances. It is not limited in dynamic aperture and shows an energy acceptance of $\pm 7\%$ restricted to 2% by the physical acceptance of the vacuum chamber at injection and $\pm 0.5\%$ by the maximum RF voltage of 0.5 MeV at 2.4 GeV.

2.2 Pre-Injector Linac

The small cross section of the booster vacuum chamber combined with the desire to minimize the electron losses throughout the injector chain, imposes tight requirements on the linac beam quality. In order to achieve clean capture into the booster RF buckets the linac has been designed to deliver an electron beam with 500 MHz structure and a single bunch purity of < 0.01 . This is achieved through a DC gun and a pulser which provides trains of 1 ns pulses at the desired repetition frequency. The 90 kV DC gun, the

Max single bunch width	1ns
Bunch train length	0.2 – 0.9 s
Max Charge	1.5nC (both modes)
Energy	>100 MeV
Pulse –pulse energy stability	<0.25%
Relative energy spread	<0.5% (rms)
Normalized emittance (1σ)	<50 mm mrad
Single bunch purity	<0.01
Repetition rate	3.0Hz, 10 Hz (max.)
RF Frequency	2.997912 GHz
Faults	<1 fault/hour

Table 2: Pre-injector linac parameters

500 MHz sub-harmonic pre-buncher and two 3 GHz travelling wave bunching sections are followed by two 5.2 m long travelling wave accelerating structures as in the DESY SBTF (S-band test facility) design [6]. The requirements on the transverse emittance and the energy spread, as well as the main linac parameters, are summarized in Table 2.

3 THE STORAGE RING

The main goal of the SLS design has been to provide very high quality sources of synchrotron radiation. The source quality (*brightness*, see Fig. 3) at constant current I is mainly determined by the electron beam quality (*low emittance*, see Table 3). The SLS has been optimized to ensure the lowest beam emittance for a given ring size.

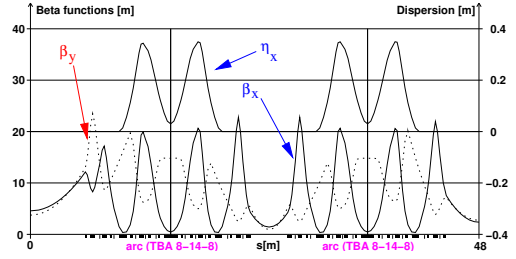


Figure 2: Storage ring optics for 1/6th of the ring ($L/2$ – TBA – S – TBA – $M/2$)

Energy	[GeV]	2.4 (2.7)
Circumference	[m]	288
RF frequency	[MHz]	500
Harmonic number		$(2^5 \times 3 \times 5 =)$ 480
Peak RF voltage	[MV]	2.6
Current	[mA]	400
Single bunch current	[mA]	≤ 10
Tunes		20.38 / 8.16
Natural chromaticity		-66 / -21
Momentum compaction		0.00065
Critical photon energy	[keV]	5.4
Natural emittance	[nm rad]	5.0
Radiation loss per turn	[keV]	512
Energy spread	$[10^{-3}]$	0.9
Damping times (h/v/l)	[ms]	9 / 9 / 4.5
Bunch length	[mm]	3.5

Table 3: Storage ring parameters

The SLS storage ring lattice consists of 12 Triple-Bend Achromats (TBA with $8^\circ/14^\circ/8^\circ$ bends) with six short (**S**) 4 m, three medium (**M**) 7 m and three long (**L**) 11 m straight sections, accounting for 27% of the ring circumference of 288 m. Two **S** sections are reserved for four cavities of 650 kV peak voltage. The injection occupies one **L** section. The lattice is designed to provide an emittance of 4.8 nm rad at 2.4 GeV with dispersion free straight sections and ≈ 4 nm rad when allowing for some dispersion. 174 quadrupoles with independent power supplies grouped into 22 families give a large tuning flexibility and 120 sextupoles in 9 families are carefully balanced to provide large dynamic apertures. The closed orbit is measured by 72 BPMs and corrected by a total number of 144 correctors in the horizontal and vertical plane; 6 skew quadrupoles grouped into 3 families around the **L** sections suppress betatron coupling. Fig. 2 depicts the optical functions for 1/6th (96 m) of the ring with two TBA and 1/2 **L**, **S** and 1/2 **M** sections. Table 3 summarizes the basic parameters of the optics presently used. An initial set of four Insertion Device (ID) based photon sources cover the energy range 10 eV to 40 keV: the high field wiggler **W61** (5-40 keV) for Materials Science (**MS**) in section **4S**, the in-vacuum undulator **U24** (8-14 keV, on loan from Spring-8) for Protein Crystallography (**PX**) in **6S**, the electromagnetic twin undulator **UE212** (8-800 eV) for Surface and Interface Spectroscopy (**SIS**) in **9L** and the Sasaki/APPLE II type twin undulator **UE56** (90 eV-3 keV) for Surface and Interface Microscopy (**SIM**) in **11M**. Fig. 3 summarizes the brightness curves for this initial set of IDs assuming storage ring operation at 2.4 GeV and 400 mA.

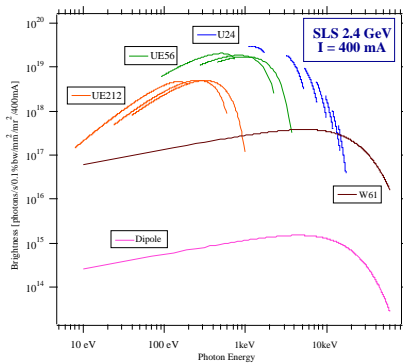


Figure 3: Brightness curves for the presently operated ID based photon sources at 2.4 GeV and 400 mA

4 COMMISSIONING OF THE INJECTORS

4.1 Pre-Injector Linac

The 100 MeV linac has been supplied as a turn-key system by ACCEL Instruments GmbH. During acceptance tests in April 2000 all parameters were demonstrated to be within specifications including the long term stability requirements (see Table 2). At the start the linac was exclusively operated in multi-bunch mode, providing a train of bunches with low charge. In order to create sharp gaps in the bunch pattern of the stored beam, an alternative operation mode, delivering highly charged single bunches, has been further optimized and is now routinely used. A transmission efficiency of 90 % through the linac has been achieved. After ± 0.5 % energy filtering 65 % of the charge remains for injection into the booster. More detailed commissioning results can be found in [1]. By April 2002 the linac had accumulated ≈ 6000 hours of operation. Reliability and reproducibility turned out to be very good. A remaining problem is the occurrence of multipactoring in the 500 MHz sub-harmonic pre-buncher resulting in a bad merging of the three S-band buckets.

4.2 Booster Synchrotron

Booster commissioning started in July 2000. On July 11 the first turn was reached without use of the 108 corrector magnets. From an “null orbit” (without corrections) excursion of 2.5 mm rms an upper limit of 0.2 mm rms for the transverse magnet alignment errors has been estimated. On August 23, the beam could be extracted at 2.4 GeV. About one month later the booster provided 1 nC (1.1 mA) at an extraction energy corresponding to a comfortable storage ring filling time to 400 mA in ≈ 3 min. A main ingredient for the successful commissioning of the booster was the digital power supply control [7] which allows a precise control of the optics parameters on the 160 ms long ramp in the 3 Hz operation mode. The system also features triggering of single cycles for top-up injection. In the course of commissioning it turned out to be more ef-

ficient to start the magnet ramp at 60 MeV and to inject the 100 MeV beam from the linac at a nonzero slope of the sinusoidal ramp for faster pass through the regime of low energy where one suffers from a reduction in lifetime due to losses by gas scattering. Due to the low emittance (9 nm rad) of the extracted beam booster-ring injection efficiencies of 100 % have been achieved when operating at nominal storage ring chromaticities, reducing to ≈ 80 % at increased chromaticities for suppression of a multi-bunch instability. After energy filtering the linac-booster transmission is close to 100 %. Due to a better compensation of eddy current induced sextupole fields, which gave rise to a head-tail instability in single bunch operation, and a more elaborate tune correction [2], losses on the ramp are negligible. By April 2002 the booster had accumulated ≈ 5500 operating hours. The booster distinguishes itself through excellent reliability and reproducibility.

5 COMMISSIONING OF THE STORAGE RING

5.1 Commissioning Milestones

In the following selected achievements (“milestones”) of the commissioning are summarized. Although scheduled for the beginning of 2001 the storage ring commissioning already started in December 2000:

Dec 13	First turn
Dec 15	First stored beam of 3 mA at 10 min lifetime
Dec 19	Lifetime of ≈ 8 h at 3 mA
2001	
Jan 19	Current of 18 mA in a relaxed optics mode
Feb 28	Current of 100 mA, operation in the optics modes: low emittance, distributed dispersion
Apr 8	First single bunch operation
Apr 26	Measurement / correction of beta functions
May 4	Closed orbit correction to μm level
Jun 5	Design current of 400 mA
Jun 23	First top-up injection
Jul 10	PX beamline operational
Jul 19	Slow global orbit feedback operational
Aug 9	First operation of the multi-bunch feedback
Aug 9	MS beamline operational
Aug 10	SIS beamline operational
Nov 21	SIM beamline operational

5.2 Lattice Calibration

Circumference Circumference measurements based on orbit measurements and sextupole centering by variation of the RF frequency confirmed the design value within 0.5 mm.

Emittances, Energy Spread, Energy Observing the X-ray part of the synchrotron radiation by means of a pin-hole camera confirmed the design value of the horizontal emittance. The vertical emittance depends on the betatron coupling and the spurious vertical dispersion gen-

erated by magnet imperfections. The integrated betatron coupling has been measured using the closest tune approach to be 0.1 % after optimization of the dedicated skew quadrupoles. Based on measured spurious vertical dispersion of ≈ 4 mm simulations predict values close to 15 pm rad which is consistent with estimates of 20-30 pm rad from Touschek lifetime measurements [8]. Nevertheless the pinhole camera gives considerably larger values around 75 pm rad. Precise measurements of the energy spread have not been carried out yet. However first decoherence measurements and the 7th harmonic photon spectrum of the undulator **U24** indicate that the energy spread is close to the design value. The beam energy has been determined to be $2.4361 \pm 5 \cdot 10^{-5}$ GeV using resonant spin depolarization of the beam [15]. A ramp from 2.4-2.7 GeV was performed without beam loss.

Working Points (WPs) The WPs in 2001 were $\nu_x=20.38/\nu_y=8.16$ providing almost equal emittances as compared to the design tunes of 20.82/8.28. Recently, even better WPs were found with 20.41/8.19 which improve injection efficiency, especially at high chromaticities and beam lifetime. The tuning range is large in both planes. ν_x has a tuning range from 20.05 to 20.495. The non-systematic 3rd integer resonance $20\frac{1}{3}$ can be crossed quickly without beam loss. The lower range limit of ν_y is 8.01. The beam is not lost at 8.5 but shows some stochastic behaviour indicating a rather narrow resonance and stabilization due to detuning.

Chromaticities The natural chromaticities $\xi_x=-66/\xi_y=-21$ have been adjusted to +1/+1 according to design and found to be +1.6/+0.5 using the model predicted sextupole settings. In order to provide beam stability at high currents, considerably larger values of $\approx +4/+4$ are required (see section 5.3). The variation of tune with momentum deviation shows excellent agreement with theory. The large negative 2nd order horizontal chromaticity makes the 3rd integer resonance $20\frac{1}{3}$ limit the energy acceptance and thus the lifetime [8].

Beta Functions Since all 174 quadrupoles are individually powered, it was straightforward to measure the average beta function at the location of each quadrupole by observing the tune as a function of the quadrupole strength. Gradient errors were fitted to the data using a Singular Value Decomposition (SVD) technique. These gradient variations were then used to correct the beta beat (rms deviation of measured beta functions with respect to the design). A beta beat of 4 % in the horizontal and 3 % in the vertical plane could be achieved [9].

5.3 Beam Current, Lifetime, Stability

When increasing the stored beam current towards the design value of 400 mA, three problems had to be overcome:

Higher Order Cavity Modes (HOMs) HOMs in the cavities, leading to sudden beam loss above some threshold current, had to be detuned by means of cavity temperature variation and HOM frequency shifters in order not to co-

incide with the multi-bunch modes [10]. Presently, beam currents up to 300 mA are routinely stored, while 400 mA requires some dedicated effort on HOM suppression.

Multi-Bunch Instability (MBI) Above some current threshold, > 50 mA, a vertical instability appears depending on the operating conditions. The MBI leads to subsequent losses of large fractions of the stored bunch pattern. Following the observations both ion trapping and resistive wall impedance effects are possible candidates for the excitation of the MBI. At the moment the MBI is suppressed by an increase of ξ_x and ξ_y to large positive values. This leads to a deterioration of the dynamic aperture and as a consequence to a reduction of the injection efficiency. A gap in the bunch pattern increases the current threshold depending on the length of the gap by destabilizing ions trapped in the electrostatic potential of the beam. The first operation tests of the transverse multi-bunch feedback system [11] lead to a significant reduction of the chromaticities needed to suppress the MBI.

Lifetime Depending on the operation mode, beam lifetime is dominated either by elastic scattering or by Touschek scattering. Variations of RF voltage, tune and single bunch current were performed to investigate the Touschek lifetime. It turned out that the Touschek lifetime is limited by the already mentioned energy acceptance restriction. Presently, a beam lifetime of ≈ 10 h is achieved with 200 mA of beam current populating 390 of the 480 buckets.

Stability The closure of the four-kicker injection bump [12] has been optimized, resulting in a residual horizontal betatron oscillation of $150 \mu\text{m}$ at maximum kick amplitude. The jitter of the stored beam due to the 3 Hz booster cycle was measured to be $\approx 0.3 \mu\text{m}$ at the location of the IDs. Phase oscillations of the RF are well below 1° over the frequency range up to 100 kHz. The amplitudes from 50 Hz and harmonic vibrations in dispersive regions are of the order of 1 micron. A slow (≈ 0.5 Hz) orbit feedback [13] stabilizes beam position and angle at the IDs to $\approx 0.6 \mu\text{m}$ and $\approx 0.3 \mu\text{rad}$. The beam intensity is kept constant at a level of ≈ 0.1 % by means of top-up injection every few tens of seconds [14]. The beam energy is stabilized to $\approx 10^{-5}$ through path length corrections applied by the feedback.

5.4 Insertion Devices

The following summarizes the installation dates of the IDs for the four initial beamlines in 2001 [16]:

Apr 10	U24 in 6S
Jul 25	Module I of UE212 in 9L
Jul 30	W61 in 4S
Oct 15	Module II of UE212
Nov 12	Module I of UE56 in 11M

Studies on the influence of the ID movement on the beam were performed. Local corrections of the IDs with dedicated correctors derived from closed orbit measurements were implemented by means of feed forward tables. As already predicted in [17], tune shift compensations are not necessary for the presently installed IDs.

5.5 Innovative Subsystems

A number of innovative subsystems have been developed for the SLS including:

Digital Power Supplies A digital control unit [7] made it possible to handle all (≈ 600) power supplies of the SLS with a fully digital control. The implementation is based on a sophisticated analogue to digital conversion and a powerful control algorithm. The tight requirements on precision and dynamic range could be fulfilled. Short/long term stabilities $< 15/100$ ppm have been demonstrated for the most demanding applications such as the main dipole circuits and the orbit corrector supplies.

Digital BPM System The commissioning of the SLS was strongly supported by a newly developed digital BPM system [18]. Applying the concept of digital receivers, it is possible to operate identical, four channel electronics in different operation modes for all accelerators of the SLS. Switching between “turn-by-turn” (high bandwidth 1 M Sample/s at medium resolution $< 20 \mu\text{m}$) and “closed orbit” (low bandwidth 4 K Sample/s at high resolution $< 1.2 \mu\text{m}$) is realized by means of EPICS based controls software [19]. The “turn-by-turn” capability has been vital at the various stages of commissioning. In the storage ring the system is able to stabilize the closed orbit with respect to a given reference to $\approx 1 \mu\text{m}$ rms as part of a orbit feedback loop and provides data for precise betatron/synchrotron tune measurements. Beam-based alignment has been performed in order to calibrate the BPMs with respect to adjacent quadrupoles [9].

Magnet Girders Quadrupole and sextupole magnets of the storage ring are pre-aligned on girders to $30 \mu\text{m}$ precision (four straight girders per TBA) whereas the dipoles form bridges between girders. Further mechanical alignment is achieved through remotely controlled girder movers, which also allows for “beam-based girder alignment” [21]. Measurements of “null orbits” with horizontal and vertical rms excursions of ≈ 2 mm and ≈ 1 mm limit the magnet misalignments on the girders to $< 50 \mu\text{m}$.

6 INITIAL OPERATION EXPERIENCE

Throughout 2002, the SLS has been exclusively operated in top-up mode for users with an average availability of 90 %. Fig. 4 shows the best week at 200 mA with current variations of 0.5 mA over a period of 4.5 days in April 2002. The slow orbit feedback stabilized the closed orbit

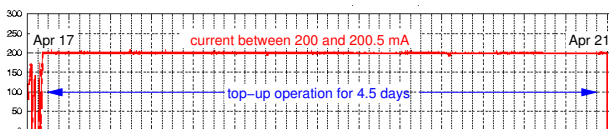


Figure 4: Top-up operation at 200 mA over 4.5 days

to $\approx 1 \mu\text{m}$ rms ($\approx 0.6 \mu\text{m}$ at the IDs) and ensured an energy stability of $\approx 10^{-5}$ over the full period. Transparent

gap operation of the IDs was guaranteed through feed forward tables and feedback. Additional losses due to top-up injection did not effect the beamline operation.

7 CONCLUSIONS

The commissioning of the SLS has been successfully completed to within design specifications and time schedule. Important design goals concerning beam current, emittance, beam stability and lifetime have been met. High availability in top-up user operation has been achieved.

8 REFERENCES

- [1] M. Pedrozzi et al., “Commissioning of the SLS Linac”, EPAC’00, Vienna 2000.
- [2] M. Muñoz, “Experience with the SLS Booster”, these proceedings.
- [3] M. Böge et al., “The SLS Accelerator Complex: An Overview”, EPAC’98, Stockholm 1998.
- [4] A. Streun et al., “Commissioning of the Swiss Light Source”, PAC’01, Chicago 2001.
- [5] A. Streun, “Achievements of the SLS Commissioning”, PSI Scientific Report 2001 Vol. VII, 2002.
- [6] M. Peiniger et al., “A 100 MeV Injector Linac for the SLS supplied by Industry”, PAC’99, New York 1999.
- [7] L. Tanner, F. Jenni, “Digitally Controlled SLS Magnet Power Supplies”, PAC’01, Chicago 2001.
- [8] A. Streun, “Beam lifetime in the SLS storage ring”, SLS Note SLS-TME-TA-2001-0191.
- [9] M. Böge et al., “Measurement and Correction of Imperfections in the SLS Storage Ring”, these proceedings.
- [10] P. Marchand et al., “Operation of the SLS RF Systems”, these proceedings.
- [11] D. Bulfone et al., “Exploitation of the Integrated Digital Processing and Analysis of the ELETTRA/SLS Transverse Multi-Bunch Feedback System”, PAC’01, Chicago 2001.
- [12] C. Gough, M. Mailand, “Septum and Kicker Systems for the SLS”, PAC’01, Chicago 2001.
- [13] M. Böge et al., “Orbit Control at the SLS Storage Ring”, these proceedings.
- [14] A. Lüdeke, M. Muñoz, “Top-Up Operation at the SLS”, these proceedings.
- [15] S. C. Leemann et al., “Beam Energy Calibration at the SLS Storage Ring”, these proceedings.
- [16] G. Ingold, T. Schmidt, “Insertion Devices: First Experiences”, PSI Scientific Report 2001 Vol. VII, 2002.
- [17] B. Singh, “Effects of Insertion Devices on the Beam Dynamics of SLS”, SLS Note SLS-TME-TA-2001-0169.
- [18] V. Schlott et al., “Commissioning of the SLS Digital BPM System”, PAC’01, Chicago 2001.
- [19] S. Hunt et al., “Control and Data Acquisition System of the SLS”, ICALEPCS’99, Trieste 1999.
- [20] S. Zelenika et al., “The SLS Storage Ring Support and Alignment Systems”, NIM A 467-468 (2001).
- [21] A. Streun et al., “Beam Stability and Dynamic Alignment at SLS”, SSILS, Shanghai 2001.